ISSN 1392–1320 MATERIALS SCIENCE (MEDŽIAGOTYRA). Vol. 15, No. 2. 2009

Composite Coatings of Alumina-based Ceramics and Stainless Steel Manufactured by Plasma Spraying

Pavel CTIBOR[1*], Helene AGEORGES[2], Karel NEUFUSS[1], Frantisek ZAHALKA[3]

[1]*Institute of Plasma Physics, ASCR, , Za Slovankou 3,182 00 Praha 8, Czech Republic*
[2]*University of Limoges, SPCTS, Av. Albert Thomas, Limoges, France*
[3]*Skoda Research, Lt.d., Tylova 57, Plzen, Czech Republic*

Received 01 August 2008; accepted 13 September 2008

Plasma spraying was used to fabricate composite (cermet) coatings from a mixture of powders of alumina-based ceramics and stainless steel. Regarding the water-stabilized plasma spray process (WSP), the two powders were mixed in the feed container, whereas a simultaneous feeding of the powders by separate injectors (co-spraying) was carried out together with the gas-stabilized plasma spray process (GSP). Both processes belong to a family of procedures known as atmospheric plasma spraying (APS), and give rise to similar coating characteristics. The complementarity of the component mixing in the two processes was demonstrated, and the mechanical properties such as microhardness and elastic modulus of the resulting composite coatings were studied. Attention was also paid to microstructural aspects connected to wear resistance.

WSP spraying of the mixed powders resulted in coatings composed of successive layers of ceramics and stainless steel, in which the relative thickness varied with the steel content. The GSP-produced cermet coating exhibited microstructures without microcracks or interconnected porosity, and such structures gave rise to good mechanical properties with respect to elastic modulus, hardness and wear resistance.

Keywords: cermet, plasma spraying, microstructure, elastic modulus, wear resistance.

INTRODUCTION

Monocomponent plasma sprayed coatings correspond less and less to the requirements of new technical applications. Instead, mixtures of two or more components are used in order to obtain a final coating with enhanced properties. Hard coatings are able to increase the resistance of metal alloys against wear, oxidation, thermal loads and corrosion, and the presence of hard particles in a coating is a mean of improving all these characteristics to a certain degree. Nevertheless, the coating also must have an elastic character; a condition that can be obtained when the matrix material is ductile enough.

Various applications of ceramic coatings include wear resistant surface covering of metallic parts. However, the wear and friction performances of these deposits are limited by morphological characteristics such as cracks. Besides, plasma-sprayed ceramic coatings can be used to impart wear resistance to the component surface but their potential is restricted by the damage caused by hard particles or asperities in erosion and abrasion wear [1, 2]. It is thus significant to add a second phase so as to eliminate these cracks and thereby to limit the brittleness of the entire coating.

Many automotive companies worldwide have developed new aluminum alloy matrix composites or protective coatings to aluminum alloys. In particular, development of wear-resistant ferrous blend coatings by plasma spraying has received growing attention because plasma spraying is the most economical and effective method applied to automotive parts such as cylinder bores, synchronizer rings, crankshafts, and piston rings among thermal spraying methods [3].

The ratio of the components in a typical mixture of ceramic and metal can be varied over a wide range. Such powders are also useful for forming bond coats, and in such cases, it is of particular interest to combine metallic and ceramic materials with different thermal expansion coefficients [4]. Alumina-steel layers can serve as an interlayer between steel substrate and ceramic top coating while alumina-steel layers should have higher hardness than commonly used bond coats, such as NiCrAlY. Microhardness of NiCrAlY is reported to be lower than 6 GPa (i. e. HV = 600) [5].

There are, in general, two simple and inexpensive ways to fabricate a composite (cermet) coating by plasma spraying. The first consists in simultaneous feeding of the two powders into the plasma jet, and the second is to feed a pre-convoluted powder as a mechanical mixture of both components. Plasma spraying of mechanical mixtures of ceramic and metallic powder was successfully realized with material combinations having a moderate difference in densities [6]. With respect to alumina and stainless steel the difference in densities is even more pronounced. To combine such different materials is rather an uncommon challenge in the plasma spray field.

It was confirmed [7] that a significant improvement of microhardness as well as wear behavior at the room temperature of Ni-based coatings can be achieved by Al_2O_3 dispersion strengthening of the matrix powder. However erosion and wear behavior at elevated temperatures of similar cermets was reported to be more problematic [8]. Also a stability of the friction coefficient versus time was worse in connection with coating with Al_2O_3 dispersion when compared to the appropriate metallic alloy [8].

Wear loss was demonstrated to decrease monotonously [3] in association with an addition from zero up to 37 vol.% of AZ40 [9] ceramic material into stainless steel

[*]Corresponding author. Tel.: + 420-266053327; fax: + 420-28586389.
E-mail address: *ctibor@ipp.cas.cz* (P. Ctibor)

AISI 316. On the same scale of the component content the microhardness monotonously increased [3].

The present paper describes the use of plasma spraying to fabricate composite (cermet) coatings from a mixture of powders of alumina-based ceramics and stainless steel. Two plasma spraying processes, i. e., a water-stabilized plasma spray process (WSP) and gas-stabilized plasma spray process (GSP), were employed and the complementarity of the component mixing in the two processes was demonstrated. Mechanical properties such as microhardness and elastic modulus of the resulting composite coatings were studied. Attention was also paid to microstructural aspects connected with wear resistance.

EXPERIMENTAL SETUPS

Plasma spraying equipment

The water-stabilized high-throughput plasma gun (WSP) [10] (see Fig. 1, a) was used for spraying a mechanical mixture of stainless steel AISI 316 and "grey alumina" (see Table 1). "Grey alumina" is a label for the composition based on Al_2O_3 with a certain amount of additives lowering the melting point and making the spray process easier. A variable steel content in the feedstock was used (see Table 2). Powders containing 0, 15, 25 and 35 weight percent of steel were sprayed on planar as well as cylindrical steel substrates (AISI 310) and striped-out to form freestanding plates or tubes. The substrates were preheated at 260 °C, the mixed powder was fed into a plasma jet 30 mm downstream of the nozzle exit and substrate stand-off distance was 350 mm. The arc current was 400 A and the corresponding power of the plasma torch was 120 kW. The powder was injected with Ar as carrier gas.

The gas-stabilized (GSP) conventional plasma gun PTF4 (SULZER METCO, Switzerland) was used for simultaneous co-spraying of stainless steel AISI 316L and "grey alumina" (see Table 1). This torch has a copper cylindrical anode nozzle while the cathode is made of thoriated tungsten (2 wt.% of Thoria) (see Fig. 1, b).

Because of the difference in melting temperatures of the oxide ceramics and stainless steel, about 2050 °C and between 1370 °C and 1400 °C, respectively, both materials were injected with two separated injectors. The first one was located inside the torch for the ceramic powder, with an internal diameter (i. d.) of 1.8 mm, while the second one used for the metallic powder was placed outside with an i. d. of 2 mm. Both injectors were positioned in the same vertical plane containing the torch axis, at 2 mm upstream and 4 mm downstream of the torch nozzle exit and at 8 mm radial distance from the anode axis.

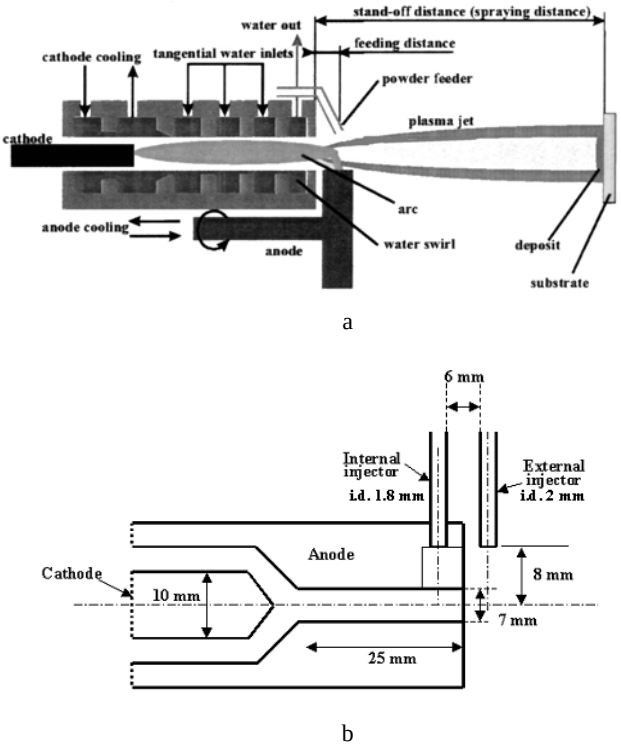

Fig. 1. WSP spraying setup (a); GSP spraying setup (b)

The powders of stainless steel and ceramics were injected with Ar as carrier gas. The flow rates were 5 slm and 4 slm, respectively, to obtain a setup where the mean particle trajectories create an angle of 3.5° with the torch axis. The substrates were disposed on a rotating sample holder the diameter of which was 90 mm. This substrate holder was rotated (tangential speed of 1 m/s) with a horizontal axis and simultaneously translated back and forth orthogonally to the plasma jet axis at a velocity of 24 mm/s, with an excursion of 160 mm, the plasma torch being stationary. The samples were cooled during plasma spraying by two compressed air cooling machined slots, avoiding the substrate heating by the plasma plume. The first one was located between the samples and the torch at 80 mm of the latter, and the second system was behind the sample holder at 20 mm from it. Basic setup parameters used for both spray procedures are summarized in Table 3.

Coating characterizations

For microscopic observation and for microhardness measurements polished cross sections of coatings were prepared. The microstructure of plasma deposits was studied by Light Microscopy (LM) and by a Scanning

Table 1. Characteristics of the powders used

Powder	Chemical composition [wt. %]	Size range [μm]	Spray technique addressed
AH	$94Al_2O_3$-$4.5TiO_2$-$1.5Fe_2O_3$	40 – 56	WSP
Steel AISI 316	62Fe-18Cr-14Ni-3Mo-2Mn	140 – 180	WSP
A300	$94Al_2O_3$-$4.5TiO_2$-$1.5Fe_2O_3$	22 – 45	GSP
Steel AISI 316L	66Fe-17Cr-13Ni-2Mo-1.7Mn	50 – 63	GSP

Table 2. Labels and characteristics of samples

Sample label	Nominal steel content [wt. %]	Spray technique	Spray specification
AH	0	WSP	external feeding
AH-5	15	WSP	spraying of mixture
AH-25	25	WSP	spraying of mixture
AH-35	35	WSP	spraying of mixture
A300	0	GSP	internal feeding
75A25st	25	GSP	co-spraying
50A50st	50	GSP	co-spraying
25A75st	75	GSP	co-spraying
316L	100	GSP	external feeding

Table 3. Plasma spraying setup parameters for sample manufacturing

Parameters	GSP	WSP
Gas flow rate Ar/H_2	45/15 NL/min	Water
Arc current	450 A to 550 A	400 A
Stand off distance	100 mm	350 mm
Substrate preheating temper.	300 °C	260 °C
Gun nozzle internal diameter	7 mm	6 mm
Substrate roughness (R_a)	8 μm ±1 μm	10 μm ±1 μm

Electron Microscopy (SEM). Image analysis software was used to define porosity, component contents and several structural features such as the thickness of steel layers in the alumina matrix when they occur. The density of deposits was measured by pycnometry and the Archimedean method, open and closed porosity were calculated. The microhardness of WSP coatings was measured with an optical microscope equipped with a Hanemann head including Vickers indenter and the used load was 1 N applied over 15 seconds. The mean value of the microhardness was calculated with 20 indentation values when monocomponent coatings were measured and 10 indentations for each component with respect to layered composite coating. For GSP coating the microhardness was determined using following conditions: the load 3 N, at the time of application about 15 seconds, for each sample 7 indents.

In our experiments with a four-point bending test of the GSP samples we have been focused not only on the measurements of elastic modulus of plasma sprayed alumina coatings but also on the behavior of elastic modulus at deformations increasing up to 0.3 %. The elastic modulus was measured using a four-point bending apparatus on an Instron 1362 mechanical testing machine. Bending was applied onto a metallic strip (120×25×2) mm covered with the coating. The special device was designed to achieve high accuracy for testing of coating-substrate plate specimens. The outer span of the supports of 94 mm was divided by inner supports into four equidistant fractions in length of 23.5 mm. To eliminate the inner stiffness of the four-point bending apparatus used, a specimen deflection was independently measured by an external strain gauge. Experimental data (displacement, strain and load) were recorded and evaluated by a special code. The usual rate of displacement was 0.0063 mm/s, maximum loads varied between 300 N and 800 N. The samples were tested 4 times from the compressive side and then 4 times from the tensile side. The elastic modulus was calculated during each test and averages are displayed.

Wear Slurry Abrasion Response (SAR) tests were performed in an Al_2O_3 suspension (particle size distribution ranging from 30 μm to 60 μm) using the apparatus based on the ASTM G75 standard (see Fig. 2). The oscillating, horizontal movement of the samples (1 in Fig. 2) in the suspension (3) was generated by a moving wheel drive (7). Stroke length was 200 mm (ASTM G75-6.2.1). The crank was rotated at 48 rpm corresponding to 2 880 r/hour (ASTM G75-6.2.1) corresponding to 5 760 revolutions per cycle. The translation speed of the sample was about 0.3 $m \cdot s^{-1}$. The wear test comprised four cycles in total distance by the sample 2 304 m. The load (5) applied was 22.2 N, corresponding to a weight of 5 lb (ASTM G75-6.2.3) and was adjusted using a dynamometer. The wear resistance was determined by the volume loss evolution versus the distance. After each cycle, the samples were ultrasonically cleaned with ethanol before being dried and weighed. Results obtained from four simultaneously tested samples were then averaged.

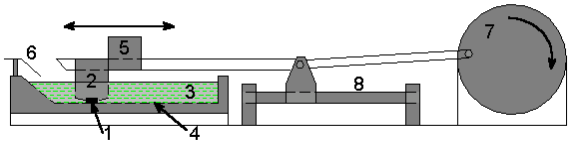

Fig. 2. Scheme of Slurry Abrasion Response (SAR) tester

Surface roughness was measured using Hommel Tester T 1000, where the trajectory was 4.8 mm long and the relative velocity of the measurement tip was 0.5 mm/s. Mean arithmetic deviation of the profile R_a, entire high of the profile R_t and maximum high of the profile R_z were determined as parameters describing the surface roughness.

Friction coefficient was evaluated using tribometer CSEM working on a principle "pin-on-disc". The "pin" used was a tungsten carbide ball having diameter 6 mm and relative velocity was 50, 100 and 150 mm/s for three radii used, 2, 4 and 6 mm, respectively, and the applied load was 10 N.

RESULTS AND DISCUSSION

Density, porosity, structure, roughness

Successive layers of alumina and stainless steel were found in the WSP coatings. The tendency to create individual layers of ceramics and metal was strongly pronounced with the AH-35 sample. The stainless steel layers became almost continuous and parallel to the substrate as soon as the steel content in the feedstock was 35 wt. %. This steel layering is an effect of feeding to the same point of plasma plume of large particles of heavy steel together with small particles of light ceramics. But the powder size was dictated by necessity for proper melting of both components.

For WPS deposits, which were freestanding bodies, density, open and closed porosity, hardness and thickness were measured. As can be seen in Table 4, the steel content has negligible influence on the porosity values. The density of the deposits is influenced by the steel content, as expected.

Table 4. Density and porosity determined by pycnometry and Archimedean weighing

Sample label	Density [g/cm^3]	Open porosity [%]	Apparent density [g/cm^3]	Porosity (open+ +closed)
AH	3.40	4.8	3.65	11.82
AH-15	3.60	5.1	3.86	12.89
AH-25	3.72	5.3	4.00	12.19
AH-35	4.00	4.6	4.29	11.52

The comparison between total porosity values (Table 4) and those measured on polished cross sections (Table 5) shows that the values are in good agreement except those related to pure ceramics. Grinding and polishing of samples caused the spurious result shown in Table 5. All samples were polished automatically at the same time and selected conditions were suitable for composite coatings but not at all for monocomponent ceramic coating. The volume content of steel in the deposits, represented by the fraction area on the microimage, is much higher than that in the feedstock. This effect could be associated with the large difference in the size of both components in the feedstock, probably resulting in a much lower deposition efficiency of ceramic powder. In the composite coating it is practically impossible to observe oxides, created from steel, by optical microscopy.

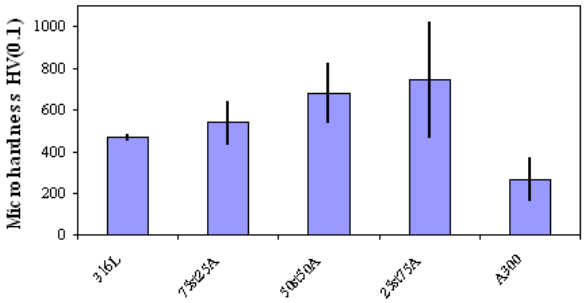

Fig. 3. Microhardness of GSP cermet coatings, *x*-axis presents the corresponding labels

Table 6 shows that the coating surfaces are smooth as follows: AH-15, AH-25**,** AH and AH-35, respectively. Also the addition of steel has a positive influence on the quality of the surface and from this point of view is also a prospect for wear performance.

Densities of GSP coatings are given in Table 7. The trend is the same as with WSP coating, the difference in absolute values is caused mainly by the fact that WSP samples were free-standing whereas GSP samples coatings on a substrate in the as-sprayed condition.

Microhardness

First, we can see in Fig. 3 that the best hardness among GSP cermet samples has a coating obtained with 25 wt.% of ceramics. The hardness increases with the increasing content of ceramics. The addition of ceramics leads to an increase of the hardness of cermet coatings because of the higher hardness of alumina. From the last column of Table 5 we can see the same trend for WSP samples. Higher values of WSP samples are caused by the lower load (1 N for WSP and 3 N for GSP) where the fact that specifically hard alumina-based ceramic exhibits higher hardness at lower load is reflected.

Elastic modulus

The GSP sample that has the highest value (see Fig. 4) is the mixture 50A50st. The mixtures 25A75st, 75A25st and also A300 have quite similar elastic modulus and finally the 316L coating has the lowest value. This enables us to understand that the elastic modulus does not depend on steel content. However it probably depends much more on the coating structure.

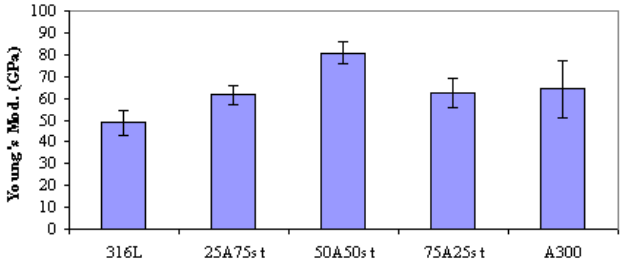

Fig. 4. Elastic modulus of GSP cermet coatings, x-axis presents the corresponding labels

Average elastic modulus *E* and the modulus of rupture MOR of WSP cermet coatings are presented in Fig. 5. An increase of steel content leads to an increase in both moduli only with the exception of 35 % steel coating and elastic modulus *E*. This exception is probably associated with the pronounced layering of this coating (see Fig. 6) which limits the coating's elasticity. The values of elastic modulus are approximately 3 times lower for WSP coating than for GSP coating, which, however, is not a rule [11 – 13] but could be associated with cohesion of the cermet components. The ratio of E of GSP versus WSP coating was in our case investigated on multicomponent coatings, so the relevance of results gained in [11 – 13] is only partial.

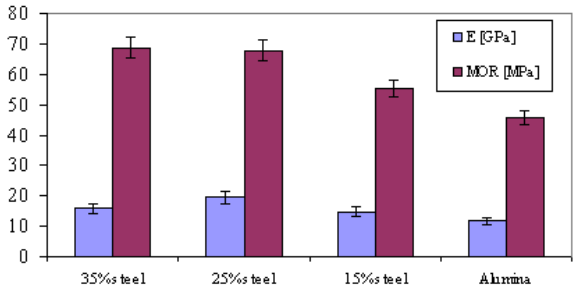

Fig. 5. Elastic modulus *E* in GPa and modulus of rupture MOR in MPa of WSP cermet coatings, *x*-axis presents the corresponding labels

Wear resistance

Wear resistance is reciprocal to the wear rate. The wear rate (see Fig. 7) decreases with ceramics content, which shows that alumina improves the wear resistance

Table 5. Image analysis of the deposits and microhardness measurements

Sample label	Steel content in the feedstock [vol. %]	Porosity of the coating [%]	Steel content in the coating [vol. %]	Thick. of steel layer [μm]	Thickness of ceramic layer [μm]	Hardness alumina	Hardness – steel	Hardness – mixture
A300	–	18.7	–	–	–	1150 ±270	–	(1150)
75A25st	7.39	9.0	23.5	No layers	No layers	1190 ±200	530 ±90	980
50A50st	12.31	10.0	26.9	No layers	No layers	1120 ±300	540 ±670	920
25A75st	17.24	12.2	39.6	37.9	97.6	1050 ±210	520 ±480	790

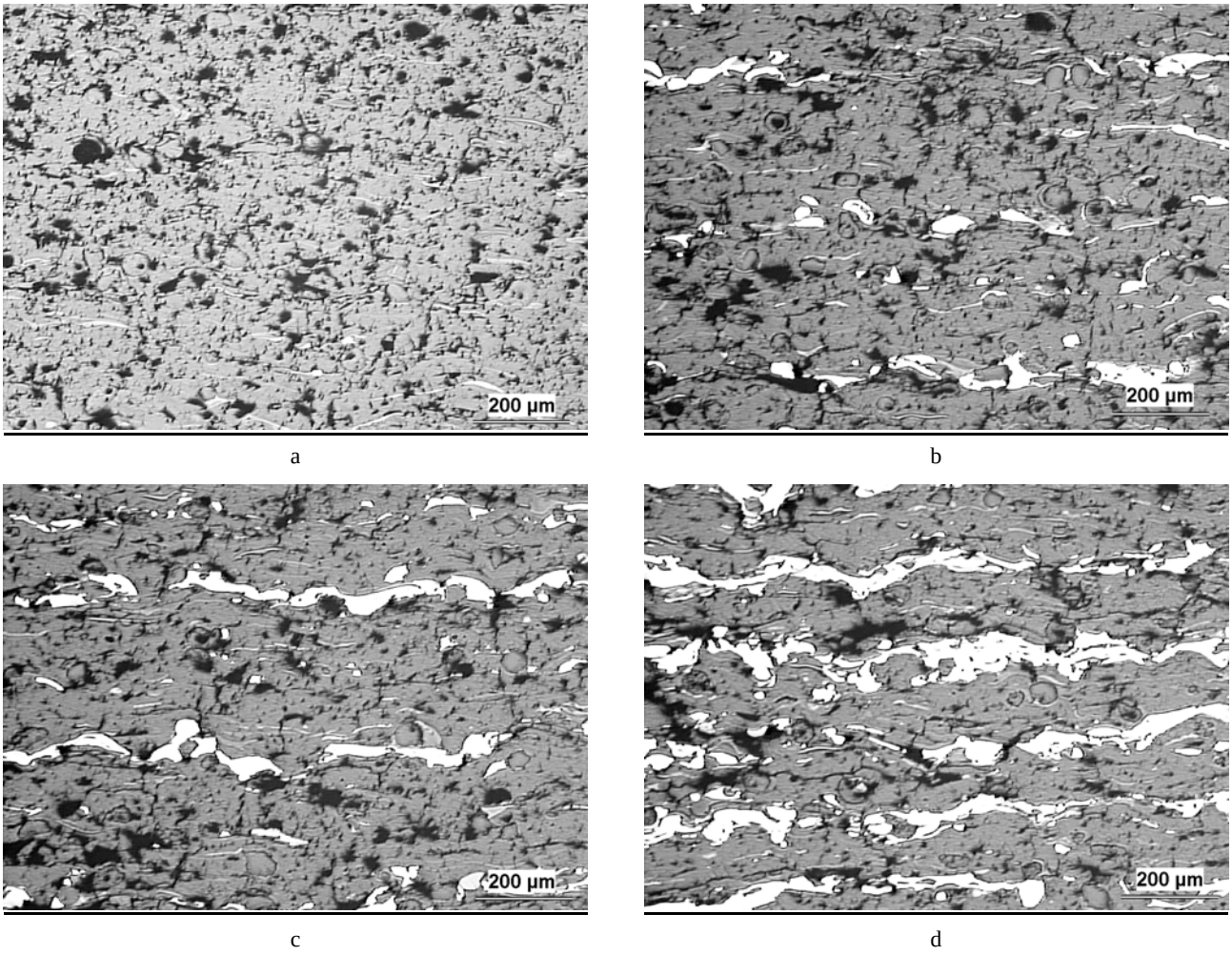

a b c d

Fig. 6. Details of the WSP coating cross sections: ceramics – grey and stainless steel – white; steel percentage is 0 (a), 15 (b), 25 (c) and 35 (d); light microscopy

of the coating. The ceramic sample A300 has an unexpectedly high wear-induced loss. This value can be attributed to a limited coating cohesion.

Table 6. Main parameters characterizing the surface roughness

Sample label	Sample	R_a [μm]	R_t [μm]	R_z [μm]
AH	AH	10.9 ±1.3	75.5 ±9.1	56.7 ±5.1
AH-15	85/15	9.0 ±0.9	69.4 ±4.5	50.2 ±4.1
AH-25	75/25	10.3 ±1.8	68.1 ±5.5	54.2 ±6.0
AH-35	65/35	11.4 ±1.2	82.6 ±16.5	61.9 ±8.3

Table 7. Density of GSP coatings used for calculation of the volume-based wear rate

Sample	Density [g/cm^3]
A300	3.7
75A25st	4.5
50A50st	5.3
25A75st	6.0
316L	6.8

Comments on the wear character of coatings: The GSP coating 25A75st is the least wear resistant among the

composite coatings. The wear was realized both by particles pulling-out and plastic deformation, fracture and subsequent removal of fragmented splats. With respect to 50A50st the deformation traces in steel splats seem to be due to residual stresses after cooling (different thermal expansion coefficients between ceramics and steel 316L). As regards the 25A75st coatings, the wear seems to act by plastic deformation more than by particles pulling-out. In the coating 75A25st the deformation traces inside steel islands were longer than in the 50A50st coating. This can be explained by the fact that the content of ceramics is even higher and, thus, the residual stresses in the steel splats are higher.

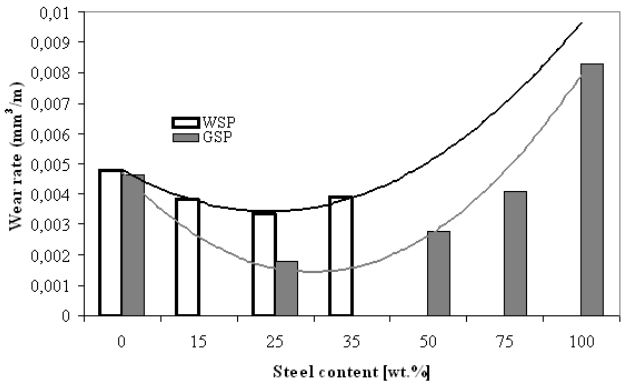

Fig. 7. Wear rate of GSP coatings

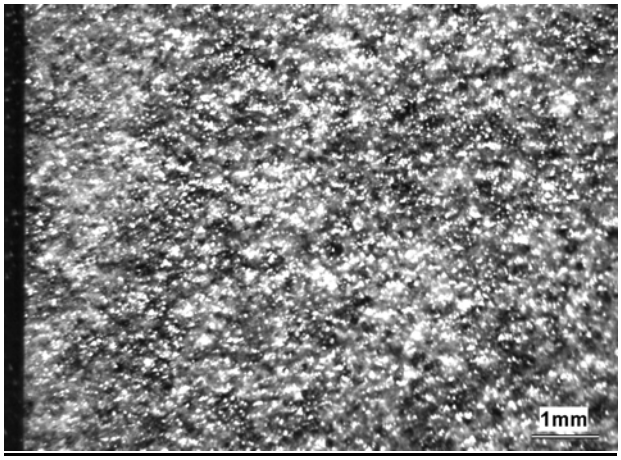

a

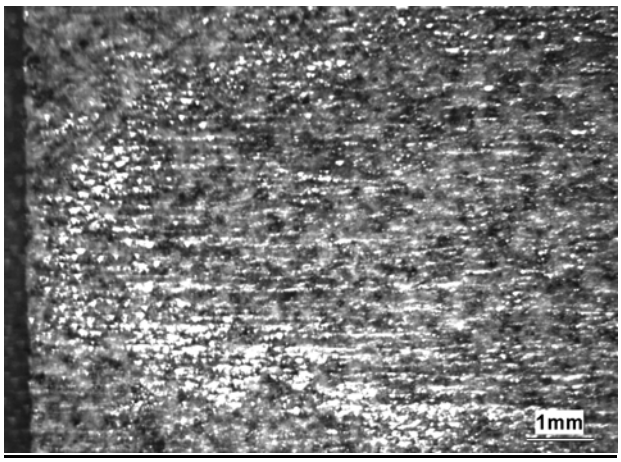

b

Fig. 8. Surface of the WSP coating with 25 % of steel in alumina before (a) and after (b) SAR test; light microscopy

The wear test had less marked impact on the appearance of the coating 75A25st surface than for the other cermets samples (Fig. 8). This observation confirms the results of the wear test (see wear rate graph in Fig. 7).

In the monocomponent ceramic coating, during the wear test some voids were formed and they are larger than the pores before the wear test. That is why we think that this coating has been worn by particles pulling-out enabled by lower cohesion of this purely ceramic coating. This surface character could explain the high wear rate of A300 coating; moreover the same trend was observed by the authors earlier at another type of cermet [14]. The trends highlighted in Fig. 7 show that for both types of coatings (GSP and WSP) the optimal composition is between 25 wt.% and 50 wt.% of steel in alumina-based ceramics.

Friction coefficient

Table 8 summarizes mean values of the friction coefficient over all three studied diameters (e. g., pin versus disc centre positions). The lowest *f* is attained by the sample AH-15, whereas the highest *f* is characteristic for the ceramic AH sample. Coefficients of both AH-25 and AH-35 samples are very similar. The dispersion of values is highest for ceramics. These facts are associated with a mainly brittle mechanism of ceramic surface degradation [15] and brings a partial answer why alumina-based ceramics is less wear resistant compare to AH-25 composition.

Table 8. Mean friction coefficient *f* values

Sample	*f*
AH	0.656 ±0.071
AH-15	0.423 ±0.021
AH-25	0.513 ±0.066
AH-35	0.524 ±0.025

CONCLUSIONS

The mixed powder (stainless steel and alumina-based ceramics) sprayed by WSP results in coatings composed of successive layers of ceramics and stainless steel relative thickness of which varies with the increasing steel content (respectively 15, 25 and 35 wt.%). The layers are contiguous and measurable by image analysis software only for 35 wt.% of steel. Such an arrangement could be promising for example to produce electric connections inside an insulating matrix. The steel content in the deposit is in any case higher than that in the feedstock, which could be caused by the large difference in melting temperature of both components in the feedstock resulting in poor deposition efficiency (improper melting) of alumina. The coatings exhibit a relatively higher porosity compared to that commonly detected in coatings made of pure ceramics and namely of pure steel.

GSP samples permitted us to study the correlation of the hardness and the microstructure to the wear resistance of the coatings. In fact, to achieve a good wear resistance, the structure has to be homogeneous and composed of well-bonded, small and hard particles. It is important to avoid interconnected porosity and microcracks in the

structure, i. e., to preserve advantages of a mixture of tough metallic particles with hard ceramics. Such a structure leads to good mechanical properties such as elastic modulus, hardness or wear resistance. For both types of coatings (GSP and WSP) the optimal composition for wear resistant coating is between 25 wt.% and 50 wt.% of steel in alumina-based ceramics.

Generally it could be pointed out that the simultaneous co-spraying of both components of feedstock powder is advantageous if a precise adjustment of the content of each component in the deposit is desirable. Also simultaneous co-spraying seems to be a more reliable way than spraying a mixed powder for production of functionally graded materials.

Acknowledgments

The Czech authors acknowledge support of the Academy of Science of the Czech Republic under project CV 1QS 200430560.

REFERENCES

1. **Tokaji, K., Ogawa, T., Hwang, J. U., Kobayashi, Y., Harada, Y.** Corrosion Fatigue Behavior of a Steel with Spray Coatings *Journal of Thermal Spray Technology* 5 (3) 1996: pp. 269 – 276.
2. **Xie, Y., Hawthorne, H. M.** The Damage Mechanisms of Several Plasma-Sprayed Ceramic Coatings in Controlled Scratching *Wear* 233 – 235 (1999) pp. 293 – 305.
3. **Song, E. P., Hwang, B., Lee, S., Kim,N. J., Ahn, J.** Correlation of Microstructure with Hardness and Wear Resistance of Stainless Steel Blend Coatings Fabricated by Atmospheric Plasma Spraying *Materials Science and Engineering A* 429 (1 – 2) 2006: pp. 189 – 195.
4. **Pawlowski, L.** The Properties of Plasma Sprayed Aluminium - Aluminium Oxide Cermets *Surface and Coatings Technology* 48 1991: pp. 219 – 224.
5. **Mishra, S. B., Chandra, K., Prakash, S.** Characterisation and Erosion Behaviour of NiCrAlY Coating Produced by Plasma Spray Method on Two Different Ni-Based Superalloys *Materials Letters* 62 (12 – 13) 2008: pp. 1999 – 2002.
6. **Gu, Y. W., Khor, K. A., Fu, Y. Q., Wang, Y.** Functionally Graded ZrO_2-NiCrAlY Coatings Prepared by Plasma Spraying Using Pre-Mixed, Spheroidized Powders *Surface and Coatings Technology* 96 (2 – 3) 1997: pp. 305 – 312.
7. **Zhao, L., Zwick, J., Lugscheider,E.** The Influence of Milling Parameters on the Properties of the Milled Powders and the Resultant Coatings *Surface and Coatings Technology* 168 (2 – 3) 2003: pp. 179 – 185.
8. **Zhao, L., Parco, M., Lugscheider, E.** Wear Behaviour of Al_2O_3 Dispersion Strengthened MCrAlY Coating *Surface and Coatings Technology* 184 (2 – 3) 2004: pp. 298 – 306.
9. **Ctibor, P., Sedlacek, J., Neufuss, K.** Influence of Chemical Composition on Dielectric Properties of Al_2O_3-ZrO_2 Plasma Deposits *Ceramics International* 29 2003: pp. 527 – 532.
10. **Hrabovsky, M.** Water Stabilized Plasma Generators *Pure & Applied Chemistry* 70 (6) 1998: pp. 1157 – 1162.
11. **Neufuss, K., Chraska, P., Kolman, B., Sampath, S., Travnicek,Z.** Properties of Plasma Sprayed Free-Standing Ceramic Parts *Journal of Thermal Spray Technology* 4 1997: pp. 434 – 438.
12. **Wallace, J. S., Ilavsky, J.** Elastic Modulus in Plasma Sprayed Deposits *Journal of Thermal Spray Technology* 7 (4) 1998: pp. 521 – 526.
13. **Harok, V., Neufuss, K.** Elastic and Inelastic Effects in Compression in Plasma-Sprayed Ceramic Coatings *Journal of Thermal Spray Technology* 1 (10) 2001: pp. 126 – 132.
14. **Ageorges, H., Ctibor, P., Medarhri, Z., Touimi, S., Fauchais, P.** Influence of the Metallic Matrix Ratio on the Wear Resistance (Dry and Slurry Abrasion) of Plasma Sprayed Cermet (Chromia/Stainless Steel) Coatings *Surface and Coatings Technology* 201 2006: pp. 2006 – 2011.
15. **Houdkova, S., Blahova, O., Enzl, R.** Abrasion Wear Rate Evaluation of Thermally Sprayed Coatings *Acta Metallurgica Slovaca* 10 2004: pp. 792 – 798.